Expression of a β-adrenergic receptor kinase 1 inhibitor prevents the development of myocardial failure in gene-targeted mice

Howard A. Rockman*†‡, Kenneth R. Chien§¶, Dong-Ju Choi*†, Guido Iaccarino‖**, John J. Hunter§, John Ross, Jr.§, Robert J. Lefkowitz**††, and Walter J. Koch‖

*Department of Medicine, University of North Carolina at Chapel Hill, Chapel Hill, NC 27599; §Department of Medicine and ¶Center for Molecular Genetics, University of California at San Diego, La Jolla, CA 92093; and Departments of ‖Surgery and **Medicine, ††Howard Hughes Medical Institute, Duke University, Durham, NC 27710

ABSTRACT   Heart failure is accompanied by severely impaired β-adrenergic receptor (βAR) function, which includes loss of βAR density and functional uncoupling of remaining receptors. An important mechanism for the rapid desensitization of βAR function is agonist-stimulated receptor phosphorylation by the βAR kinase (βARK1), an enzyme known to be elevated in failing human heart tissue. To investigate whether alterations in βAR function contribute to the development of myocardial failure, transgenic mice with cardiac-restricted overexpression of either a peptide inhibitor of βARK1 or the β₂AR were mated into a genetic model of murine heart failure ($MLP^{-/-}$). *In vivo* cardiac function was assessed by echocardiography and cardiac catheterization. Both $MLP^{-/-}$ and $MLP^{-/-}/\beta_2AR$ mice had enlarged left ventricular (LV) chambers with significantly reduced fractional shortening and mean velocity of circumferential fiber shortening. In contrast, $MLP^{-/-}/\beta ARKct$ mice had normal LV chamber size and function. Basal LV contractility in the $MLP^{-/-}/\beta ARKct$ mice, as measured by LV dP/dtmax, was increased significantly compared with the $MLP^{-/-}$ mice but less than controls. Importantly, heightened βAR desensitization in the $MLP^{-/-}$ mice, measured *in vivo* (responsiveness to isoproterenol) and *in vitro* (isoproterenol-stimulated membrane adenylyl cyclase activity), was completely reversed with overexpression of the βARK1 inhibitor. We report here the striking finding that overexpression of this inhibitor prevents the development of cardiomyopathy in this murine model of heart failure. These findings implicate abnormal βAR-G protein coupling in the pathogenesis of the failing heart and point the way toward development of agents to inhibit βARK1 as a novel mode of therapy.

One of the most important mechanisms for rapidly regulating β-adrenergic receptor (βAR) function is agonist-stimulated receptor phosphorylation by G protein-coupled receptor kinases (GRKs) resulting in decreased sensitivity to further catecholamine stimulation (1, 2). βARK1 is a member of the multigene GRK family that regulates a wide variety of receptors that couple to heterotrimeric G proteins (1, 2). Desensitization of agonist-occupied receptors by the cytosolic βAR kinase (βARK1) requires a membrane-targeting event before its activation and receptor phosphorylation, which is mediated by a direct physical interaction between residues within the carboxyl terminus of βARK1 and the dissociated membrane-anchored βγ subunits of G proteins (Gβγ) (3, 4).

Heart failure is a disease characterized by left ventricular (LV) dysfunction associated with a complex of symptoms that relate to inadequate perfusion of tissues and pulmonary congestion. Although the fundamental molecular abnormality that causes this progressive deterioration in cardiac function is unknown, one of the leading candidates is abnormal βAR signaling. Chronic human heart failure is characterized by severely attenuated βAR signaling, resulting from diminished receptor number and impaired receptor function (5), leading to inotropic subsensitivity and impaired exercise tolerance (6). Increased levels of βARK1, found in failing human heart tissue, have been postulated to account for impaired receptor function in response to agonist stimulation (7, 8). In animal models of heart disease, prominent βAR desensitization recently has been shown to be associated with heightened levels of βARK1 (9, 10). Our findings in transgenic mice that overexpress different members of the GRK family demonstrate how the up-regulation of βARK1 in the diseased heart could markedly alter βAR function through receptor desensitization (9, 11, 12). Importantly, inhibition of myocardial βARK1 activity because of cardiac-targeted expression of a peptide inhibitor of βARK1 (βARKct) led to enhanced contractility demonstrating the critical role of βARK1 in normal heart function (11). The βARKct is composed of the last 195 aa of βARK1, which contains the binding site for Gβγ and competes with endogenous βARK1 for Gβγ membrane translocation and activation (11).

A limitation in addressing mechanistic pathways in the setting of heart failure has been the lack of a well characterized model of murine heart failure that has fidelity to the human condition (13). Recently, a genetic model of murine-dilated cardiomyopathy has been described that involves ablation of a muscle-restricted gene that encodes the muscle LIM protein ($MLP^{-/-}$) (14). Our goal was to determine whether abnormalities in βAR signaling in the failing heart play a causative role in the progressive deterioration in cardiac function and whether reversal of these alterations can lead to improvement of cardiac function. To accomplish this, our strategy was to mate transgenic mice with cardiac-targeted overexpression of either the βARKct (11) or the β₂AR (15) into the $MLP^{-/-}$ model of heart failure.

METHODS

Experimental Animals. MLP$^{-/-}$ mice were mated with transgenic mice with cardiac-targeted overexpression of the βARKct (11). F1 pups generated from an $MLP^{-/-} \times \beta ARKct(t/t)$ homozygote cross were mated to create the $MLP^{+/-}/\beta ARKct(t/0)$ double heterozygote (where t represents the presence of a transgene). F2 offspring generated from a $MLP^{-/-} \times MLP^{+/-}/\beta ARKct(t/0)$ double heterozygote mating generated mice that were $MLP^{-/-}$ and $MLP^{-/-}/\beta ARKct(t/0)$ with the remainder of the pups heterozygous for MLP with and without the βARKct transgene. F3 offspring were generated by back-

Abbreviations: LV, left ventricular; βAR, β-adrenergic receptor; βARK1, βAR kinase; GRK, G protein-coupled receptor kinase; MLP, muscle LIM protein.
†H.A.R. and D.-J.C. contributed equally to this work.
‡To whom reprint requests should be addressed at: Department of Medicine, CB#7075, University of North Carolina at Chapel Hill, Chapel Hill, NC 27599-7075. e-mail: hrockman@med.unc.edu.

crossing a $MLP^{-/-}/\beta ARKct(t/0)$ mouse into the $MLP^{-/-}$ parent to generate $MLP^{-/-}$ and $MLP^{-/-}/\beta ARKct(t/0)$ littermates. A similar strategy was used to generate $MLP^{-/-}/\beta_2AR(t/0)$ gene-targeted mice. The genotype of the various gene-targeted crosses was determined by PCR on genomic DNA isolated from tail biopsies as described previously (11, 14, 15). Expression of the $\beta ARKct$ peptide in hearts of $MLP^{-/-}/\beta ARKct$ mice was confirmed by immunoblotting using a polyclonal antibody directed against the C terminus of $\beta ARK1$. The animals in this study were handled according to approved protocols and the animal welfare regulations of the University of North Carolina at Chapel Hill, Duke University, and the University of California at San Diego.

Transthoracic Echocardiography. Echocardiography was performed in anesthetized mice (2.5% avertin, 14 μl/g intraperitoneally) by using an Apogee CX echocardiograph (Interspec-ATL, Bothell, WA) as described previously (16). Echocardiography was performed in nonlittermate control $MLP^{+/+}$ mice by using a different anesthesia (mixture of 100 mg/kg ketamine and 5 mg/kg xylazine, i.p.), which is associated with a lower heart rate and therefore mean velocity of circumferential fiber shortening (mean Vcf) (16).

Cardiac Catheterization. Hemodynamic evaluation in intact mice was performed as described previously (9). Mice were anesthetized with a mixture of ketamine (100 mg/kg) and xylazine (2.5 mg/kg) and, after endotracheal intubation, were connected to a rodent ventilator. After bilateral vagotomy, the left carotid artery was cannulated with a flame-stretched PE-50 catheter connected to a modified P-50 Statham transducer (17). A 1.4 French (0.46 mm) high-fidelity micromanometer catheter (Millar Instruments, Houston, TX) was inserted into the right carotid and advanced retrograde into the LV. Hemodynamic measurements were recorded at baseline and 45–60 sec after injection of incremental doses of isoproterenol (9).

Adenylyl Cyclase Activity and βAR Binding. Adenylyl cyclase activity and βAR binding were performed from myocardial sarcolemmal membranes (9, 11). For cyclase activity, membranes (30–40 μg protein) were incubated for 15 min at 37°C with $[\alpha\text{-}^{32}P]ATP$ under basal conditions or indicated agonists and cAMP was quantified (9, 11). Total βAR density was determined by incubating 25 μg of sarcolemmal membranes with a saturating concentration of $[^{125}I]$cyanopindolol and 20 μM alprenolol to define nonspecific binding (9, 11).

Immunoblotting. Immunodetection of myocardial levels of $\beta ARK1$ was performed on cytosolic extracts after immunopre-

cipitation by using a monoclonal $\beta ARK1/2$ antibody as described previously (9, 11, 18). The ≈ 80-kDa $\beta ARK1$ protein was visualized with the mAb raised against an epitope within the carboxyl terminus of $\beta ARK1$ and chemiluminescent detection of anti-mouse IgG conjugated with horseradish peroxidase (ECL, Amersham). GRK activity was measured in myocardial membranes by using rhodopsin-enriched rod outer segment membranes as an *in vitro* substrate and $[\gamma\text{-}^{32}P]ATP$ as described previously (9, 11, 18). $[^{32}P]$ incorporation into rhodopsin was quantified by using a using a Molecular Dynamics PhosphorImager (9, 11, 18).

Histological Analysis of Gene-Targeted Mouse Hearts. Unfixed myocardial cryosections were obtained and histological staining of myocytes was done with Masson's trichrome by standard protocols (14).

Statistical Analysis. Data were expressed as mean ± SEM. To test for statistical differences in echocardiographic data between all groups, a one-factor ANOVA was performed accompanied by a Newman–Keuls post hoc analysis when appropriate. Hemodynamic data were analyzed with a repeated-measures ANOVA, and post hoc analysis with regard to differences in mean values between the groups at a specific dose was conducted with a Newman–Keuls test. Cyclase activity was analyzed with a repeated-measures ANOVA. βAR density and NaF stimulation were determined with a one-factor ANOVA. A Student's *t* test was used to test differences in the level of myocardial $\beta ARK1$.

RESULTS

To investigate whether abnormalities in βAR signaling are responsible for the progressive deterioration in cardiac function in the failing heart, we used a strategy whereby transgenic mice with cardiac-targeted overexpression of either the $\beta ARKct$ (11) or the β_2AR (15) were mated into the $MLP^{-/-}$ model of heart failure. *In vivo* cardiac function in these novel, dual gene-targeted mice was assessed by echocardiography. $MLP^{-/-}$ mice have enlarged cardiac chambers with depressed function as shown by the increase in LV end-diastolic and end-systolic dimension associated with a reduction in fractional shortening (FS) and mean Vcf (Table 1 and Fig. 1*A*). Cardiac overexpression of the β_2AR in the MLP-deficient background did not influence the development of the dilated cardiomyopathic phenotype, because cardiac chambers remained enlarged whereas FS and mean Vcf continued to be depressed compared with $MLP^{-/-}$ littermates (Table 1 and Fig. 1*A*). In striking contrast, cardiac-targeted $\beta ARK1$ inhibition through overexpression of the $\beta ARKct$ prevented the deteriora-

Table 1. Transgene overexpression in MLP-deficient mice: *In vivo* echocardiographic assessment

	$MLP^{-/-a}$, $n = 12$	$MLP^{-/-}/\beta_2AR$, $n = 9$	$MLP^{-/-b}$, $n = 7$	$MLP^{-/-}/\beta ARKct$, $n = 9$	$MLP^{+/+}$, $n = 16$
LVEDD, mm	4.86 ± 0.29	4.78 ± 0.27	4.89 ± 0.24	3.74 ± 0.22†	3.94 ± 0.09†
LVESD, mm	3.84 ± 0.30	3.94 ± 0.31	3.97 ± 0.28	2.43 ± 0.22*	2.47 ± 0.08*
FS, %	22.3 ± 2.3	18.5 ± 3.6	19.3 ± 2.2	35.8 ± 2.4*	37.4 ± 1.2*
SEPth, mm	0.67 ± 0.04	0.56 ± 0.05	0.56 ± 0.03	0.59 ± 0.04	0.67 ± 0.02
PWth, mm	0.66 ± 0.04	0.58 ± 0.05	0.58 ± 0.04	0.58 ± 0.05	0.68 ± 0.02
HR, beats/min	437 ± 28	517 ± 44	483 ± 36	474 ± 28	258 ± 12‡
mean Vcf, circ/s	4.06 ± 0.35	3.74 ± 0.65	4.11 ± 0.57	7.73 ± 0.81*	4.64 ± 0.20‡
mean Vcfc, circ/s	1.51 ± 0.14	1.32 ± 0.21	1.48 ± 0.22	2.88 ± 0.25*	2.24 ± 0.12*‡
BW, g	36.3 ± 3.0	34.2 ± 2.5	33.6 ± 1.7	29.9 ± 1.8	33.8 ± 1.8
Mean age at echo, months	7.3 ± 0.8	5.1 ± 0.7	5.3 ± 0.1	6.9 ± 0.7	3.4 ± 0.1

Analysis of *in vivo* cardiac size and function by echocardiography in gene-targeted mice. Mating of transgenic mice with cardiac overexpression of the β_2AR or a a $\beta ARKct$ into the MLP-deficient background resulted in mice homozygous for the MLP gene ablation and heterozygous for either the β_2AR ($MLP^{-/-}/\beta_2AR$) or the $\beta ARKct$ ($MLP^{-/-}/\beta ARKct$), $MLP^{-/-a}$ and $MLP^{-/-b}$ are littermates for the β_2AR and $\beta ARKct$ cross, respectively. $MLP^{+/+}$ are adult nonlittermate wild-type mice of the same genetic background that were used as controls. LVEDD, left ventricular end diastolic dimension; LVESD, left venrtricular end systolic dimension; HR, heart rate; FS, fractional shortening calculated as (LVEDD − LVESD)/LVEDD × 100; SEPth, septal wall thickness; PWth, posterior wall thickness; mean Vcf, mean velocity of circumferential fiber shortening; mean Vcfc, heart rate-corrected mean Vcf; BW, body weight. *$P < 0.0005$, †$P < 0.01$, $MLP^{-/-}/\beta ARKct$ and $MLP^{+/+}$ vs. either $MLP^{-/-b}$ or $MLP^{-/-a}$; ‡$P < 0.01$, MLP(+/+) vs. $MLP^{-/-}/\beta ARKct$. The $MLP^{-/-}/\beta ARKct$ and $MLP^{-/-a}$ mice were significantly older than the other groups. ($P < 0.05$). $MLP^{+/+}$ mice underwent echocardiography with a different anesthesia, accounting for the slower heart rate and therefore a lower mean Vcf (16). However, for the echocardiographic parameters measured, no significant differences in any of the other variables were found between the $MLP^{-/-}/\beta_2AR$ and their $MLP^{-/-a}$ littermates, or between the $MLP^{-/-a}$ and $MLP^{-/-b}$ littermate groups. Therefore, for subsequent analysis of echocardiographic data, the $MLR^{-/-}$ groups were pooled.
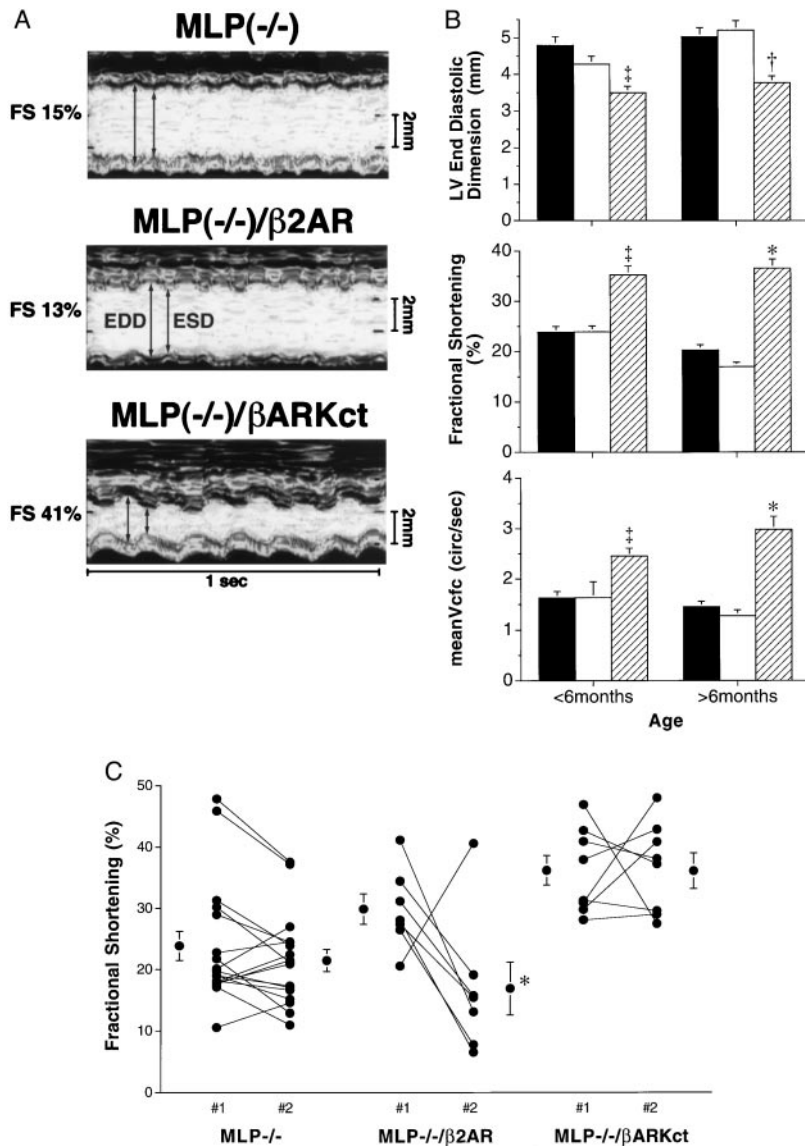
FIG. 1.   Analysis of cardiac function by echocardiography. (*A*) Transthoracic M-mode echocardiographic tracings in a $MLP^{-/-}$ (*Top*), $MLP^{-/-}/\beta_2AR$ (*Middle*), and a $MLP^{-/-}/\beta ARKct$ mouse (*Bottom*). Left ventricular dimensions are indicated by the double-sided arrows. EDD, end diastolic dimension; ESD, end systolic dimension. Both the $MLP^{-/-}$ and $MLP^{-/-}/\beta_2AR$ mice have chamber dilatation with reduced wall motion indicating depressed cardiac function, whereas chamber size and cardiac function are normal in the $MLP^{-/-}/\beta ARKct$ mouse. (*B*) Echocardiographic findings in mice under 6 months of age: $MLP^{-/-}$ (solid bar, mean age 4.1 ± 0.4 months, $n = 18$), $MLP^{-/-}/\beta_2AR$ (open bar, mean age 4.3 ± 0.4 months, $n = 8$), and $MLP^{-/-}/\beta ARKct$ (hatched bar, mean age 4.7 ± 0.7 months, $n = 9$); and more than 6 months of age: $MLP^{-/-}$ (solid bar, mean age 7.0 ± 0.5 months, $n = 17$), $MLP^{-/-}/\beta_2AR$ (open bar, mean age 7.3 ± 0.7 months, $n = 3$), and $MLP^{-/-}/\beta ARKct$ (hatched bar, mean age 6.9 ± 0.77 months, $n = 8$). Data represent serial echocardiograms in the same mouse at different ages except if the mouse died during the interval between studies. *, $P < 0.005$; †, $P < 0.01$; ‡, $P < 0.05$ $MLP^{-/-}/\beta ARKct$ vs. $MLP^{-/-}$ and $MLP^{-/-}/\beta_2AR$, one-factor ANOVA. (*C*) Change in cardiac function over a 2.5- to 3-month period in the three groups of gene-targeted mice. #1, early study (mean age, 3.9 months); #2, later study (mean age, 6.4 months). For comparison, normal values obtained in $MLP^{+/+}$ mice are shown in Table 1.

tion in cardiac function (Table 1 and Fig. 1*A*). In $MLP^{-/-}/$ $\beta ARKct$ mice compared with age-matched $MLP^{-/-}$ littermates, LV end-diastolic and end-systolic dimensions were significantly smaller, whereas FS and mean Vcf were significantly higher, indicating preserved cardiac function (Table 1 and Fig. 1*A*).

To determine whether changes in ventricular function were time-dependent, serial echocardiography was performed in the three groups of gene-targeted mice. $MLP^{-/-}$ mice and $MLP^{-/-}/\beta_2AR$ under 6 months of age have enlarged LV chambers with depressed cardiac function (reduced FS and mean Vcfc) (Fig. 1*B*). In contrast, $MLP^{-/-}/\beta ARKct$ mice under 6 months of age have normal LV chamber size and function (Fig. 1*B*). This beneficial effect of the $\beta ARKct$ on cardiac function persisted as the mice grew older, whereas little change and even some deterioration occurred in the $MLP^{-/-}$ and $MLP^{-/-}/\beta_2AR$ mice (Fig. 1*B*). Individual data points are plotted for FS to determine whether a serial change in cardiac function occurred over a 3-month period (Fig. 1*C*). Whereas $MLP^{-/-}$ animals had reduced FS that did not change over time, the presence of additional cardiac β_2ARs ($MLP^{-/-}/\beta_2AR$) resulted in deterioration of FS in the majority of mice. In contrast, FS was preserved in the $MLP^{-/-}/\beta ARKct$ mice and remained in the normal range over the 3-month study interval (Fig. 1*C*).

To determine whether overexpression of the $\beta ARKct$ can reverse the marked βAR desensitization associated with the

$MLP^{-/-}$ mice, we performed cardiac catheterization in intact anesthetized mice. LV contractility (assessed by LV dP/dtmax) at baseline in the $MLP^{-/-}/\beta ARKct$ mice was modestly but significantly increased compared with the $MLP^{-/-}$, but was less than nonlittermate wild-type $MLP^{+/+}$ control mice (Fig. 2*A*). However, the abnormal response to isoproterenol stimulation, characteristic of the $MLP^{-/-}$ animals, was reversed completely with $\beta ARKct$ overexpression (Fig. 2 *A* and *B*). This response to isoproterenol was essentially identical to that in the wild-type $MLP^{+/+}$ mice and is consistent with a mechanism of $\beta ARK1$ inhibition that preserves normal βAR-G protein coupling (Fig. 2 *A* and *B*). Similarly, the increase in heart rate from baseline in response to βAR stimulation was preserved in the $MLP^{-/-}/$ $\beta ARKct$ mice although basal heart rate was lower than in wild-type mice (Fig. 2*C*). Furthermore, the markedly elevated LV end diastolic pressure in the $MLP^{-/-}$ mice (an indication of the severe impairment of cardiac function in these animals) was normalized by chronic $\beta ARKct$ expression (Fig. 2*D*). The minimal first derivative of LV pressure, LV dP/dtmin, also was enhanced in the $MLP^{-/-}/\beta ARKct$ compared with the $MLP^{-/-}$ mice at baseline ($-3,964 \pm 420$ vs. $-2,634 \pm 140$, mmHg/sec, $P < 0.005$) but was significantly less than that in wild-type mice ($-7,411 \pm 986$, mmHg/s, $P < 0.0005$). This relationship persisted with isoproterenol administration (data not shown). Baseline LV systolic pressure was similar in the $MLP^{-/-}/\beta ARKct$ animals
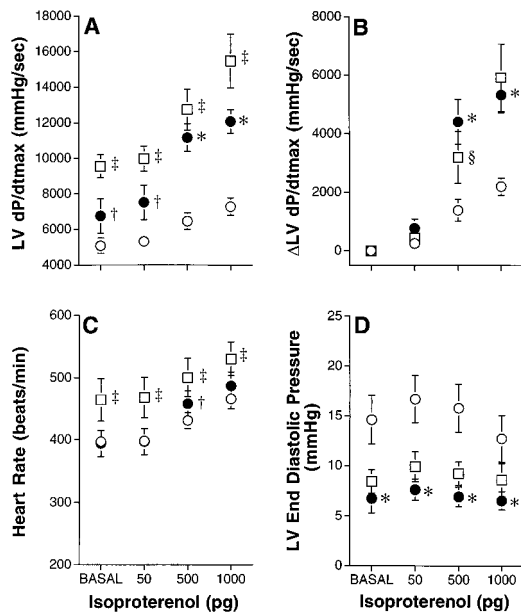
FIG. 2. *In vivo* assessment of β-AR responsiveness. Cardiac catheterization was performed in intact, anesthetized mice. Parameters are shown at baseline and after progressive infusion of isoproterenol in $MLP^{-/-}$ (○), $n = 15$, $MLP^{-/-}/\beta$ARKct (●), $n = 7$, and wild-type $MLP^{+/+}$ (□), $n = 6$, mice. (*A*) Maximal first derivative of LV pressure, LV dP/dtmax. (*B*) The difference from baseline for LV dP/dtmax, ΔLV dP/dtmax. (*C*) Heart rate. (*D*) LV end diastolic pressure. ∗, $P < 0.0005$; †, $P < 0.01$ $MLP^{-/-}/\beta$ARKct vs. $MLP^{-/-}$; ‡, $P < 0.005$; §, $P < 0.05$ wild-type $MLP^{+/+}$ vs. $MLP^{-/-}/\beta$ARKct. A significant between-group main effect in response to isoproterenol was found for LV dP/dtmax, $P < 0.00001$ (*A*); heart rate, $P = 0.05$ (*C*); and LV end diastolic pressure, $P < 0.05$ (*D*). The pattern of change between groups was statistically significantly for LV dP/dtmax, $P < 0.00001$ (*A*) and ΔLV dP/dtmax, $P < 0.00001$ (*B*).

compared with the $MLP^{-/-}$ mice (90 ± 4 vs. 96 ± 4 mmHg), but was lower than that in the MLP wild-type mice (128 ± 10 mmHg). Hemodynamic analysis could not be performed in the $MLP^{-/-}/\beta_2$AR mice because survival was considerably shortened and did not allow for an adequate number of animals.

βAR density and adenylyl cyclase activity were determined in cardiac membranes prepared from the various gene-targeted lines. βAR density was reduced significantly by 54% in the $MLP^{-/-}$ compared with wild-type hearts and was associated with marked attenuation of isoproterenol-stimulated adenylyl cyclase activity, indicating severe impairment of βAR coupling (Table 2). Although βAR density also was reduced in $MLP^{-/-}/\beta$ARKct compared with wild-type mice, isoproterenol-stimulated adenylyl cyclase activity was enhanced significantly and intermediate between wild-type and MLP-deficient mice (Table 2). Importantly, fold increase in membrane cyclase activity with isoproter-
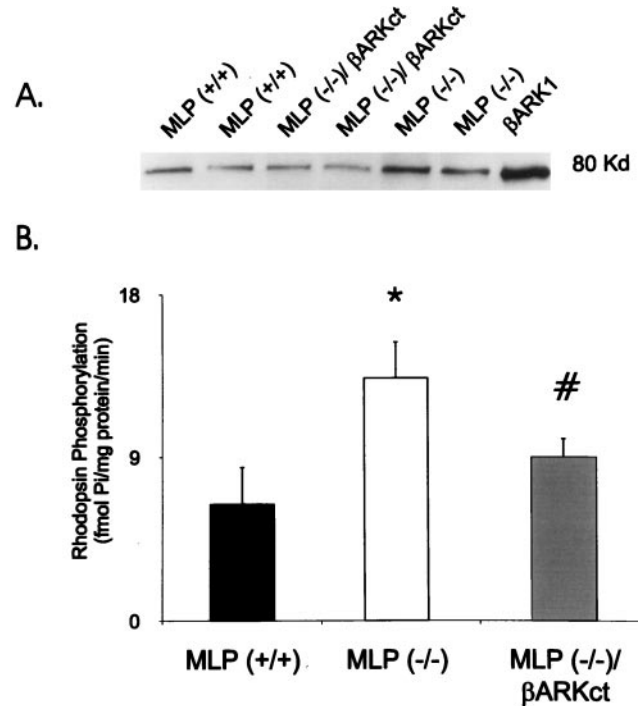

FIG. 3. Assessment of myocardial βARK1 levels and activity. (*A*) βARK1 protein levels of myocardial extracts were determined by protein immunoblotting. Shown is a representative experiment with two hearts from each gene-targeted mouse. Similar results were obtained in two more hearts in each group. βARK1 protein levels were ≈2-fold higher in the $MLP^{-/-}$ hearts compared with $MLP^{+/+}$ hearts ($P < 0.05$) whereas myocardial βARK1 levels in the $MLP^{-/-}/\beta$ARKct hearts were not significantly different than wild-type hearts. (*B*) Rhodopsin-enriched rod outer segment membranes were used as a substrate for membrane myocardial GRK activity and ^{32}P incorporation was quantified from dried gels. The data represent a sample size of four to six hearts in each group. ∗, $P < 0.05$ vs. $MLP^{+/+}$; #, $P < 0.03$ vs. $MLP^{-/-}$.

enol stimulation in the $MLP^{-/-}/\beta$ARKct hearts was 2.8 vs. 2.6 in the wild-type hearts and 1.7 in the $MLP^{-/-}$ hearts, indicating restitution toward normal G protein coupling. These biochemical findings are completely concordant with the *in vivo* data (Fig. 2) and indicate that the functional uncoupling of βARs seen in the failing $MLP^{-/-}$ hearts can be prevented with chronic overexpression *in vivo* of the βARKct. This is also consistent with the LV weight data obtained after terminal hemodynamic study where a significant decrease in LV mass in the $MLP^{-/-}/\beta$ARKct hearts ($n = 8$) compared with $MLP^{-/-}$ hearts ($n = 15$) was observed (LV weight to tibia length ratio, 6.5 ± 0.3 vs. 7.8 ± 0.3 mg/mm, $P < 0.02$). LV mass in the $MLP^{-/-}/\beta$ARKct hearts was slightly, but not significantly, higher than that in the control hearts ($MLP^{+/+}$, 5.5 ± 0.3 mg/mm, $n = 6$).

Table 2. βAR signaling characteristics

	βAR density, fmol/mg membrane protein	Adenylyl cyclase activty, % NaF stimulation	
		Basal	ISO, 10^{-4} M
$MLP^{-/-}$	16.6 ± 1.9, $n = 11$	2.7 ± 0.1, $n = 5$	4.5 ± 0.7, $n = 5$
$MLP^{-/-}/\beta$ARKct	23.0 ± 5.4, $n = 6$	2.8 ± 0.7, $n = 5$	7.8 ± 1.5†‡, $n = 5$
$MLP^{+/+}$	36.0 ± 4.3∗, $n = 6$	5.2 ± 0.6§, $n = 5$	13.4 ± 0.7†, $n = 5$

NaF values in pmol per min per mg: $MLP^{-/-}$, 33.0 ± 2.8; $MLP^{-/-}/\beta$ARKct, 32.8 ± 1.6; $MLP^{+/+}$, 49.7 ± 4.8 ($P < 0.02$, $MLP^{+/+}$ vs. $MLP^{-/-}/\beta$ARKct and $MLP^{-/-}$). ∗$P < 0.02$, $MLP^{+/+}$ vs. $MLP^{-/-}/\beta$ARKct and $MLP^{-/-}$; †$P < 0.005$, ISO vs. basal for $MLP^{-/-}/\beta$ARKct and $MLP^{+/+}$; ‡$P < 0.02$, ISO $MLP^{-/-}/\beta$ARKct vs. ISO $MLP^{+/+}$ and ISO $MLP^{-/-}$; §$P = 0.07$ basal $MLP^{+/+}$ vs. basal $MLP^{-/-}/\beta$ARKct and basal $MLP^{-/-}$. ISO, isoproterenol.
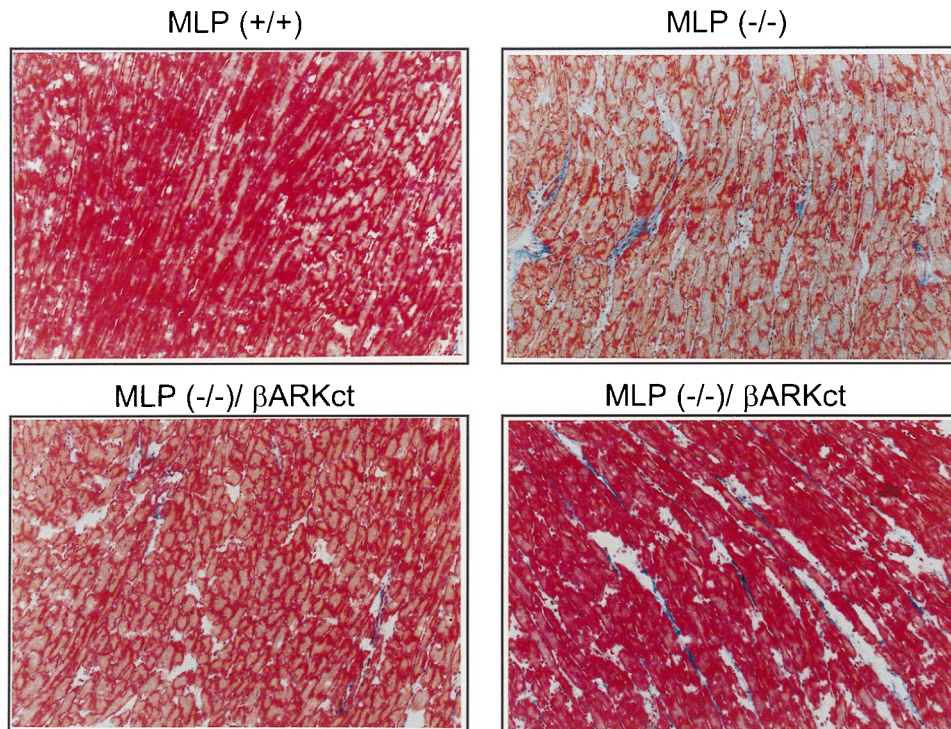
Fig. 4.   Histological analysis of gene-targeted mouse hearts. Representative sections stained with Masson's trichrome are shown from $MLP^{+/+}$ and $MLP^{-/-}$ hearts and two $MLP^{-/-}$/βARKct hearts.

Because βARK1 levels and activity are enhanced in human heart failure, we sought to determine whether myocardial βARK1 levels are increased in the $MLP^{-/-}$ mouse, which could contribute to the marked βAR uncoupling observed. Myocardial βARK1 levels were assessed by immunoprecipitation of soluble heart extracts. Cytosolic βARK1 levels were ≈2-fold higher in the hearts of $MLP^{-/-}$ animals compared with $MLP^{+/+}$ animals (Fig. 3*A*). Furthermore, we measured enzyme activity in extracts from myocardial membranes, because this is where βARK1 exerts its regulatory actions. We found membrane GRK activity to be significantly increased and parallel to the protein data (Fig. 3*B*). Immunoblotting for a second GRK found in the heart, GRK5, revealed no difference in expression between the different lines of mice (data not shown), indicating that the increase in membrane kinase activity can be accounted for by translocated βARK1 to the membrane. Taken together, these data show that chronic myocardial expression of the βARKct eliminates development of the severe heart failure phenotype and prevents the up-regulation of βARK1 as demonstrated by both protein immunoblotting and GRK activity (Fig. 3 *A* and *B*).

The deleterious effects of β$_2$AR overexpression in the $MLP^{-/-}$ mice is demonstrated further by the marked adverse effect on survival. Cumulative survival probability for $MLP^{-/-}$/β$_2$AR mice ($n = 11$) was shortened significantly such that over a 9-month follow-up period the probability of survival was approximately 12% compared with 80% for the $MLP^{-/-}$ mice ($n = 19$; $P < 0.0001$, Mantel–Haenszel χ^2 statistic, $MLP^{-/-}$/β$_2$AR vs. $MLP^{-/-}$). Over the same time period only 1 of 10 $MLP^{-/-}$/βARKct mice died, which occurred at 7 months of age, and did not differ significantly from the $MLP^{-/-}$ mice. These data clearly demonstrate that enhancing βAR signaling through marked overexpression of β$_2$ARs in this murine model of myocardial failure has deleterious consequences that are accompanied by persistent cardiac chamber enlargement, progressive deterioration in cardiac function, and diminished survival. In contrast, reversal of βAR desensitization through chronic overexpression of a βARK1 inhibitor essentially prevents the development of heart failure in $MLP^{-/-}$ mice.

We also examined the hearts of these gene-targeted mice histologically and found that the characteristic fibrosis found in the $MLP^{-/-}$ hearts (14) did not seem to lessen because of the presence of the βARKct (Fig. 4). This is not surprising and suggests that the histopathological changes in the $MLP^{-/-}$ hearts are a result of the absence of the cytoskeletal MLP protein and are not a result of the dilated cardiomyopathy *per se*.

DISCUSSION

The above echocardiographic and hemodynamic findings suggest that GRK-mediated βAR desensitization plays a causative role in the development of heart failure in this animal model. Moreover, they indicate the potential for novel therapeutic strategies that aim to modulate the activity level of myocardial βARK1 during the course of the cardiomyopathic process. We have chosen to use a genetic-based model of dilated cardiomyopathy through targeted disruption of the muscle LIM protein gene, which closely resembles the phenotype of human dilated cardiomyopathy (14). The MLP is a conserved positive regulator of myogenic differentiation, and recent findings suggest that it may act as a molecular adapter to promote protein assembly along the actin-based cytoskeleton. Hearts from MLP-deficient mice are characterized by marked disruption of cardiomyocyte architecture (14). Human heart failure also is a disease of cardiac muscle characterized by alterations in cardiomyocyte shape (19), cytoskeletal abnormalities (20), and βAR signaling (5), which supports our use of the MLP-deficient mouse as a model system to study underlying mechanisms in this disease.

Although abnormalities in βAR signaling have been postulated to promote cardiac dysfunction in the failing heart, other hypotheses have been suggested, which include altered Ca^{2+} availability (21), impaired ability of the L-type Ca^{2+} channel to activate sarcoplasmic reticulum Ca^{2+} release (22), and abnormalities in myocyte cytoskeleton such as microtubular polymerization (23). Although the precise mode of action by which overexpression of the βARKct provides this salutary effect is not clear, it is unlikely to be a result of a nonspecific effect of transgene overexpression because cardiac overexpression of a β$_2$AR transgene in the

MLP-deficient background had no effect on the heart failure phenotype. The strikingly opposite phenotypes observed with overexpression of the β_2AR and overexpression of the βARKct suggests that marked chronic enhancement of βAR signaling by markedly increasing receptor number is not sufficient to prevent deterioration in cardiac function. In contrast, reversal of β_1AR desensitization through overexpression of a βARK1 inhibitor acts to restore normal G protein coupling of the endogenous uncoupled β_1ARs. The lack of a beneficial effect with β_2AR transgene overexpression may in part be related to the extraordinarily high levels of receptor overexpression in those mice (15) or perhaps a result of different signaling properties of the β_2AR compared with the β_1AR (24). Furthermore, β_2AR overexpression in this model leads to constant maximal signaling (15), whereas βARKct overexpression preserves myocardial βAR responsiveness to endogenous catecholamine stimulation (11). The deleterious effect of chronic βAR stimulation in the $MLP^{-/-}/\beta_2$AR mice is consistent with the experience from clinical studies using oral inotropic agents in severe heart failure (25). Our data suggest that restoring normal control of β_1AR signaling by inhibiting enhanced desensitization is an important mechanism to prevent the progressive deterioration in cardiac function in this model of heart failure. Interestingly, it has been shown recently that treatment with the βAR antagonist, carvedilol, can improve survival in human heart failure (26). Although the mechanism(s) is not known, an intriguing basis for this beneficial effect of βAR antagonism may be the reduction of desensitization through lowering of βARK1 levels (ref. 10; G.I., E. D. Tomhave, R.J.L., and W.J.K., unpublished results).

Because the βARKct peptide inhibits βARK1 activity via $G_{\beta\gamma}$ sequestration, we cannot definitively exclude the possibility that inhibition of other $G_{\beta\gamma}$-dependent pathways contributes to the improved cardiac status of the $MLP^{-/-}/\beta$ARKct animals. However, several lines of evidence argue strongly for inhibition of βARK1 activity being the primary mechanism. First, the $MLP^{-/-}/\beta$ARKct mice have increased βAR-coupling efficiency demonstrated by the increased isoproterenol-stimulated adenylyl cyclase activity and *in vivo* cardiac function, which clearly suggests inhibition of desensitization, just as would be expected for βARK1 inhibition. Second, overexpression of the βARKct does not prevent the development of cardiac hypertrophy in response to pressure overload but reverses βAR desensitization (9), suggesting that other signaling pathways critical for the hypertrophic phenotype are unaffected by the βARKct. Third, mice heterozygous for the βARK1 gene deletion, which possess 50% less βARK1 enzyme compared with wild-type animals, have a cardiac phenotype of enhanced contractility and sensitivity to βAR agonists (H.A.R., S. A. Akhter, D.-J.C., M. Jaber, R.J.L., M. G. Caron, and W.J.K. unpublished results) essentially identical to the βARKct-overexpressing animals (11). Finally, when the βARKct transgenic mice were crossed into the βARK1 heterozygous knockout background, this led to a further enhancement of cardiac function and isoproterenol responsiveness, which was associated with a stepwise decrement in $G_{\beta\gamma}$-dependent βARK1 activity (H.A.R., S. A. Akhter, D.-J.C., M. Jaber, R.J.L., M. G. Caron, and W.J.K. unpublished results).

Other known actions of $G_{\beta\gamma}$ (27, 28) such as activation of the $I_{k.ach}$ channel, adenylyl cyclase, PLCβ1–3, and MAP kinase appear not to be relevant in this situation. The $I_{k.ach}$ channel is located in atrial and not ventricular tissue and would not be expected to directly alter contractility (27, 29). The isoforms of adenylyl cyclase that are regulated by $G_{\beta\gamma}$ (I, II, IV) are not found in the heart (28). PLCβ is not activated by myocardial βARs (27). Finally, *in vivo* activation of MAP kinase does not affect contractility (30). Taken together, these data strongly suggest that the striking effects of the βARKct indeed are mediated primarily through βARK1 inhibition and restored βAR coupling and not through effects on other $G_{\beta\gamma}$-dependent pathways.

We do not, however, currently know whether the beneficial effect of βARK1 inhibition also is mediated in part through reduction of desensitization of G protein-coupled receptors other than βARs such as, for example, the angiotensin (18) or endothelin receptor. However, if this were the case, an opposite result would be expected. Inhibition of βARK1 by the βARKct would increase signaling through these pathways, whereas previous studies have demonstrated the marked benefit of blocking both angiotensin (31) and endothelin (32) signaling in heart failure.

The evidence we present here demonstrates the critical role that chronic βAR desensitization plays in the development of heart failure and the importance of preserving normal βAR coupling. That the inhibition of a single molecule (βARK1) can have such a dramatic effect on a cardiac phenotype caused by a structural abnormality (MLP deficiency) is surprising and indicates that βARK1 inhibition may offer a novel therapeutic target in heart failure with the potential to have significant impact on this disease.

1. Inglese, J., Freedman, N. J., Koch, W. J. & Lefkowitz, R. J. (1993) *J. Biol. Chem.* **268,** 23735–23738.
2. Lefkowitz, R. J. (1993) *Cell* **74,** 409–412.
3. Pitcher, J. A., Inglese, J., Higgins, J. B., Arriza, J. L., Casey, P. J., Kim, C., Benovic, J. L., Kwatra, M. M., Caron, M. G. & Lefkowitz, R. J. (1992) *Science* **257,** 1264–1267.
4. Koch, W. J., Inglese, J., Stone, W. C. & Lefkowitz, R. J. (1993) *J. Biol. Chem.* **268,** 8256–8260.
5. Bristow, M. R., Ginsburg, R., Minobe, W., Cubicciotti, R. S., Sageman, W. S., Lurie, K., Billingham, M. E., Harrison, D. C. & Stinson, E. B. (1982) *N. Engl. J. Med.* **307,** 205–211.
6. Colucci, W. S., Denniss, A. R., Leatherman, G. F., Quigg, R. J., Ludmer, P. L., Marsh, J. D. & Gauthier, D. F. (1988) *J. Clin. Invest.* **81,** 1103–1110.
7. Ungerer, M., Bohm, M., Elce, J. S., Erdmann, E. & Lohse, M. J. (1993) *Circulation* **87,** 454–463.
8. Lohse, M. J., Krasel, C., Winstel, R. & Mayor, F., Jr. (1996) *Kidney Int.* **49,** 1047–1052.
9. Choi, D. J., Koch, W. J., Hunter, J. J. & Rockman, H. A. (1997) *J. Biol. Chem.* **272,** 17223–17229.
10. Ping, P., Gelzer-Bell, R., Roth, D. A., Kiel, D., Insel, P. A. & Hammond, H. K. (1995) *J. Clin. Invest.* **95,** 1271–1280.
11. Koch, W. J., Rockman, H. A., Samama, P., Hamilton, R. A., Bond, R. A., Milano, C. A. & Lefkowitz, R. J. (1995) *Science* **268,** 1350–1353.
12. Rockman, H. A., Koch, W. J., Milano, C. A. & Lefkowitz, R. J. (1996) *J. Mol. Med.* .
13. Chien, K. R. (1996) *J. Clin. Invest.* **97,** 901–909.
14. Arber, S., Hunter, J. J., Ross, J., Jr., Hongo, M., Sansig, G., Borg, J., Perriard, J.-C., Chien, K. R. & Caroni, P. (1997) *Cell* **88,** 393–403.
15. Milano, C. A., Allen, L. F., Rockman, H. A., Dolber, P. C., McMinn, T. R., Chien, K. R., Johnson, T. D., Bond, R. A. & Lefkowitz, R. J. (1994) *Science* **264,** 582–586.
16. Tanaka, N., Dalton, N., Mao, L., Rockman, H. A., Peterson, K. L., Gottshall, K. R., Hunter, J. J., Chien, K. R. & Ross, J., Jr. (1996) *Circulation* **94,** 1109–1117.
17. Rockman, H. A., Ross, R. S., Harris, A. N., Knowlton, K. U., Steinhelper, M. E., Field, L. J., Ross, J., Jr., & Chien, K. R. (1991) *Proc. Natl. Acad. Sci. USA* **88,** 8277–8281.
18. Rockman, H. A., Choi, D. J., Rahman, N. U., Akhter, S. A., Lefkowitz, R. J. & Koch, W. J. (1996) *Proc. Natl. Acad. Sci. USA* **93,** 9954–9959.
19. Gerdes, A. M., Kellerman, S. E., Moore, J. A., Muffly, K. E., Clark, L. C., Reaves, P. Y., Malec, K. B., McKeown, P. P. & Schocken, D. D. (1992) *Circulation* **86,** 426–430.
20. Schaper, J., Froede, R., Hein, S., Buck, A., Hashizume, H., Speiser, B., Friedl, A. & Bleese, N. (1991) *Circulation* **83,** 504–514.
21. Gwathmey, J. K., Copelas, L., MacKinnon, R., Schoen, F. J., Feldman, M. D., Grossman, W. & Morgan, J. P. (1987) *Circ. Res.* **61,** 70–76.
22. Gomez, A. M., Valdivia, H. H., Cheng, H., Lederer, M. R., Santana, L. F., Cannell, M. B., McCune, S. A., Altschuld, R. A. & Lederer, W. J. (1997) *Science* **276,** 800–806.
23. Tsutsui, H., Ishihara, K. & Cooper, G., IV (1993) *Science* **260,** 682–687.
24. Xiao, R. P., Hohl, C., Altschuld, R., Jones, L., Livingston, B., Ziman, B., Tantini, B. & Lakatta, E. G. (1994) *J. Biol. Chem.* **269,** 19151–19156.
25. Packer, M., Carver, J. R., Rodeheffer, R. J., Ivanhoe, R. J., DiBianco, R., Zeldis, S. M., Hendrix, G. H., Bommer, W. J., Elkayam, U., Kukin, M. L., *et al.* (1991) *N. Engl. J. Med.* **325,** 1468–1475.
26. Packer, M., Bristow, M. R., Cohn, J. N., Colucci, W. S., Fowler, M. B., Gilbert, E. M. & Shusterman, N. H. (1996) *N. Engl. J. Med.* **334,** 1349–1355.
27. Clapham, D. E. & Neer, E. J. (1993) *Nature (London)* **365,** 403–406.
28. Tang, W. J. & Gilman, A. G. (1992) *Cell* **70,** 869–872.
29. Nair, L. A., Inglese, J., Stoffel, R., Koch, W. J., Lefkowitz, R. J., Kwatra, M. M. & Grant, A. O. (1995) *Circ. Res.* **76,** 832–838.
30. Hunter, J. J., Tanaka, N., Rockman, H. A., Ross, J., Jr., & Chien, K. R. (1995) *J. Biol. Chem.* **270,** 23173–23178.
31. Pitt, B., Segal, R., Martinez, F. A., Meurers, G., Cowley, A. J., Thomas, I., Deedwania, P. C., Ney, D. E., Snavely, D. B. & Chang, P. I. (1997) *Lancet* **349,** 747–752.
32. Sakai, S., Miyauchi, T., Kobayashi, M., Yamaguchi, I., Goto, K. & Sugishita, Y. (1996) *Nature (London)* **384,** 353–355.